ORIGINAL CONTRIBUTION

Vinexin-β protects against cardiac hypertrophy by blocking the Akt-dependent signalling pathway

Ke Chen · Lu Gao · Yu Liu · Yan Zhang · Ding-Sheng Jiang · Xiang Wei · Xue Hai Zhu · Rui Zhang · Yingjie Chen · Qinglin Yang · Noriyuki Kioka · Xiao-Dong Zhang · Hongliang Li

Abstract Cardiac hypertrophy is the heart's response to hypertrophic stimuli and is associated with increased mortality. Vinexin-β is a vinculin-binding protein that belongs to a family of adaptor proteins and mediates signal transduction and actin cytoskeleton organisation. A previous study has shown that Vinexin-β is ubiquitously expressed and that it is highly expressed in the heart. However, a critical role for Vinexin-β in cardiac hypertrophy has not been investigated. Therefore, to examine the role of Vinexin-β in pathological cardiac hypertrophy, we used Vinexin-β knockout mice and transgenic mice that over-express human Vinexin-β in the heart. Cardiac hypertrophy was induced by aortic banding (AB). The extent of cardiac hypertrophy was quantitated by echocardiography and pathological and molecular analyses of heart samples. Our results demonstrated that Vinexin-β overexpression in the heart markedly attenuated cardiac hypertrophy, fibrosis, and cardiac dysfunction, whereas loss of Vinexin-β exaggerated the pathological cardiac remodelling and fibrosis response to pressure overload. Further analysis of the in vitro and in vivo signalling events indicated that beneficial Vinexin-β effects were associated with AKT signalling abrogation. Our findings demonstrate for the first time that Vinexin-β is a novel mediator that protects against cardiac hypertrophy by blocking the AKT signalling pathway.

Keywords Vinexin-β · AKT · Cardiac remodelling · Hypertrophy

K. Chen, L. Gao and Y. Liu are co-first authors.

Electronic supplementary material The online version of this article (doi:10.1007/s00395-013-0338-0) contains supplementary material, which is available to authorized users.

K. Chen · X.-D. Zhang (✉)
College of Life Sciences, Wuhan University,
Wuhan 430072, People's Republic of China
e-mail: zhangxd@whu.edu.cn

L. Gao
Department of Cardiology, Institute of Cardiovascular Disease,
Union Hospital, Tongji Medical College, Huazhong University
of Science and Technology, Wuhan, People's Republic of China

Y. Liu · Y. Zhang · D.-S. Jiang · H. Li (✉)
Department of Cardiology, Renmin Hospital of Wuhan
University, Jiefang Road 238,
Wuhan 430060, People's Republic of China
e-mail: lihl@whu.edu.cn

Y. Zhang · D.-S. Jiang · R. Zhang · H. Li
Cardiovascular Research Institute of Wuhan University,
Jiefang Road 238, Wuhan 430060, People's Republic of China

X. Wei · X. H. Zhu
Department of Thoracic and Cardiovascular Surgery,
Tongji Hospital, Tongji Medical College,
Huazhong University of Science and Technology,
Wuhan 430030, People's Republic of China

Y. Chen
Cardiovascular Division, University of Minnesota,
Minneapolis, MN 55455, USA

Q. Yang
Department of Nutrition Sciences, University of Alabama
at Birmingham, Birmingham, AL 35294-3360, USA

N. Kioka
Division of Applied Life Sciences, Graduate School
of Agriculture, Kyoto University, Sakyo, Kyoto, Japan

Introduction

Cardiac hypertrophy is the heart's response to a variety of extrinsic and intrinsic stimuli, and it is characterised by an increase in myocardial mass and accumulation of extracellular matrix [20, 25, 26]. Although cardiac hypertrophy is an initial adaptive response of the myocardium, it ultimately progresses to heart failure, which is associated with high rates of mortality and morbidity [17, 27, 34]. Over the past few decades, a series of studies have elucidated the signalling transduction pathways that promote the hypertrophic response, however, the mechanisms that antagonise these pathways are not yet completely known.

Vinexin was first identified as a vinculin-binding protein, and it localises to cell–cell junctions and focal adhesion sites [21]. It belongs to an adaptor protein family that comprises vinexin, c-Cbl associated protein (CAP)/ponsin, and Arg-binding protein 2(ArgBP2). Proteins in this family are involved in both signal transduction and actin cytoskeletal organisation [22]. Vinexin is expressed as three isoforms, including Vinexin α, β, and γ [21, 30]. All three isoforms share a common C-terminal sequence that contains three SH3 domains, while Vinexin α and γ have an additional SoHo domain. The first and second SH3 domains in Vinexin-β mediate vinculin binding, whereas the third SH3 domain binds Sos, an important signalling molecule of the Ras pathway. Vinexin-β is ubiquitously expressed, with its highest levels in the heart [21]. The structural features of Vinexin-β are similar to other adaptor and scaffold proteins, e.g., Grb2 and p130cas, which are important modulators in signalling pathways and hypertrophy [23, 43]. These observations raise the possibility that Vinexin-β plays an important role in regulating cardiac hypertrophy. Herein, we examined the effects of Vinexin-β overexpression or deficiency on cardiac hypertrophy and failure in response to chronic pressure overload. The results presented in this study demonstrate that transgenic mice with cardiac-specific overexpression of Vinexin-β were resistant to aortic banding (AB)-triggered cardiac remodelling through the inactivation of the AKT signalling pathway, whereas Vinexin-β knockout mice were sensitive to the cardiac hypertrophic response induced by AB. These findings suggest that Vinexin-β is a pivotal modulator of cardiac remodelling and failure in response to chronic pressure overload.

Methods and materials

Materials

The following primary antibodies were used in our experiments. Anti-Vinexin-β (ab68222) was purchased from Abcam. Anti-ERK1/2(#4695), anti-phospho-ERK1/2$^{Thr202/Thr204}$ (#4370), anti-MEK1/2 (#9122), anti-FOXO3A (#2497), anti-phospho-MEK1/2$^{Ser217/221}$ (#9154), anti-P38 (#9212), anti-phospho-P38$^{Thr180/Thr182}$ (#4511), anti-phospho-JNK1/2 (#4668), anti-JNK1/2 (#9258), anti-AKT (#4691), anti-phospho-AKT^{Ser473} (#4060), anti-phospho-FOXO3A$^{Ser318/321}$ (#9465), anti-GSK3β (#9315), anti-phospho-GSK3βS9 (#9322), and anti-α-actinin (#3134) were purchased from Cell Signalling Technology. Anti-Flag (F3165) was purchased from Sigma-Aldrich, anti-Myc from Roche, and anti-GAPDH (MB001) from Bioworld Technology. The Akt inhibitor LY294002 was obtained from Cell Signalling technology (Cat NO: 9901). The BCA protein assay kit was purchased from Pierce. IRDye® 800CW-conjugated secondary antibodies (LI-COR Biosciences) were used in our immunoblotting analysis. Foetal calf serum (FCS) was obtained from Hyclone. Cell culture reagents and all other reagents were obtained from Sigma.

Animal models and animal surgery

The animal protocol was approved by the Animal Care and Use Committee of the Renmin Hospital of Wuhan University, China. All surgeries and subsequent analyses were performed in a blinded fashion. Full-length human Vinexin-β cDNA was cloned downstream of the cardiac myosin heavy chain (α-MHC) promoter. Transgenic mice were then produced by microinjection of the α-MHC-Vinexin-β construct into fertilised mouse embryos (C57BL/6 background). Four independent transgenic lines were established. Transgenic mice were identified by PCR analysis of tail genomic DNA. Primers were designed as follows: 5′-ATCTCCCCC ATAAGAGTTTGAGTC-3′ and 5′-GGGTGGGTCTTCCA AGGTCCAGTCC-3′. The expected size for the amplification product was 694 bp. The Vinexin-β knockout mouse model was generously provided by the RIKEN Bio Resource Center (BRC) through the National Bio Resource Project of the MEXT, Japan.

AB was performed as described previously [20, 25, 40, 42]. Doppler analysis was carried out to ensure that adequate constriction of the aorta had been induced. The internal diameter and wall thickness of the left ventricle (LV) were assessed by echocardiography at the indicated times after surgery or infusion. The hearts, lungs, and tibiae of the killed mice were collected and weighed for calculating the following ratios: heart weight (HW)/body weight (BW) (mg/g), HW/tibial length (TL) (mg/mm), and lung weight (LW)/BW (mg/g).

Blood pressure and echocardiography

A microtip catheter transducer (SPR-839, Millar Instruments, and Houston, Texas) was inserted into the right

carotid artery and advanced into the left ventricle. After stabilisation for 15 min, the pressure signals and heart rate were recorded continuously using an ARIA pressure–volume conductance system coupled to a Powerlab/4SP A/D converter, stored, and displayed on a personal computer as described previously [20, 25]. Echocardiography was performed using a MyLab 30CV ultrasound (Biosound Esaote Inc.) with a 10-MHz linear array ultrasound transducer. The LV was assessed in both parasternal long- and short-axis views at a frame rate of 120 Hz. End-systole or end-diastole was defined as the phase in which the smallest or largest area of LV, respectively, was obtained. The LV end-systolic diameter (LVESD) and LV end-diastolic diameter (LVEDD) were measured from the LV M-mode trace, which had a sweep speed of 50 mm/s at the mid-papillary muscle level.

Plasmid constructs

EGFP-myc-Akt plasmid was constructed by subcloning the coding region of human AKT into the *Bam*HI and *Xho*I sites of the pSico-EGFP-myc-C1 vector. Specifically, human AKT cDNA was PCR amplified using the primers Akt-F and Akt-R, digested with *Bam*HI and *Xho*I, and then ligated into the pSico-EGFP-myc-C1 vector. pSico-Flag-Vinexin-β plasmid was constructed by subcloning the coding region of mouse Vinexin-β into the *Bam*HI and *Xho*I sites of the pSico-Flag-C1 vector. Specifically, mouse Vinexin-β cDNA was PCR amplified using the primers Vinexin-F and Vinexin-R, digested with *Bam*HI and *Sal*I, and then ligated into the pSico-Flag-C1 vector. All plasmids were verified by sequencing. The primers for PCR: Vinexin-F, CGCGGATCCATGGCTGATGGAGGAAGC CC; Vinexin-R, ACGCGTCGACTCACACCGGGGCAAC GTAAT; Akt-F, ACGCGTCGACGGATCCGAATTCAT GAGCGACGTGGCTATTGTGAA; Akt-R, ACGCCAAT TGCTCGAGTCAGGCCGTGCCGCTGGCCGA.

Co-immunoprecipitation assays

To analyse the interaction of Akt and Vinexin-β in vivo, co-immunoprecipitation assays were performed using HEK293T cells. HEK293T cells were lysed in RIPA buffer containing a $1\times$ protease inhibitor cocktail (Roche). The cell lysates were incubated with the specified antibody and Protein G Agarose (Roche) overnight at 4 °C. The resins were collected by centrifugation and then washed four times with NETN buffer. The bound proteins were eluted with loading buffer (3 % SDS, 1.5 % β-mercaptoethanol, 8 % glycerol, 0.01 % Coomassie Brilliant Blue G-250, 150 mM Tris–HCl, pH 7.0), separated by SDS-PAGE, and immunoblotted with the appropriate antibodies.

Western blotting

Cardiac tissue and cultured cardiomyocytes were lysed in RIPA buffer. Protein extracts were isolated as described previously [25]. Fifty microgram of the protein extracts was used for SDS-PAGE. The proteins were then transferred to nitrocellulose membranes and probed with various antibodies. After incubation with an IRDye® 800CW-conjugated secondary antibody, the signals were visualised using an Odyssey Imaging System. Specific protein expression levels on the same nitrocellulose membrane were normalised to that of GAPDH for the total cell lysate.

Histological analysis

Hearts were excised, placed immediately in a 10 % potassium chloride solution to ensure that they were stopped in diastole, washed with saline solution, and placed in 10 % formalin. The hearts were sectioned transversely and close to the apex to visualise the left and right ventricles. Several sections (4- to 5-μm thick) were prepared and stained with haematoxylin–eosin (HE) for histopathology or picrosirius red (PSR) for collagen deposition analysis and then visualised by light microscopy. To determine the cross-sectional area (CSA) of the myocytes, the HE-stained sections were used. A single myocyte was measured using a quantitative digital analysis imaging system (Image-Pro Plus 6.0). Between 100 and 200 myocytes in the left ventricles were outlined in each group.

Recombinant adenoviral vectors and cultured neonatal rat cardiac myocytes

To overexpress Vinexin-β, we used replication-defective adenoviral vectors encompassing the entire rat Vinexin-β cDNA coding region under the control of the cytomegalovirus (CMV) promoter. An adenoviral vector encoding the *GFP* gene was used as a control. To knock down Vinexin-β expression, three rat shVinexin-β constructs were obtained from SABiosciences (KR51403G). Next, we generated three Ad-shVinexin-β adenoviruses and selected the one that produced a significant downregulation of endogenous Vinexin-β expression for further experiments. Ad-shRNA was the non-targeting control. We infected cardiac myocytes with Ad-Vinexin-β, Ad-GFP, Ad-shVinexin-β, or Ad-shRNA at a multiplicity of infection (MOI) of 10, which resulted in transgene expression without toxicity in 95–100 % of the cells.

Neonatal rat cardiomyocytes (NRCMs) were prepared as described previously [20, 25]. Briefly, cells from the hearts of 1- to 2-day-old Sprague–Dawley rats were seeded at a density of 1×10^6 cells/well in plating medium, which consisted of F10 medium supplemented with 10 % FCS
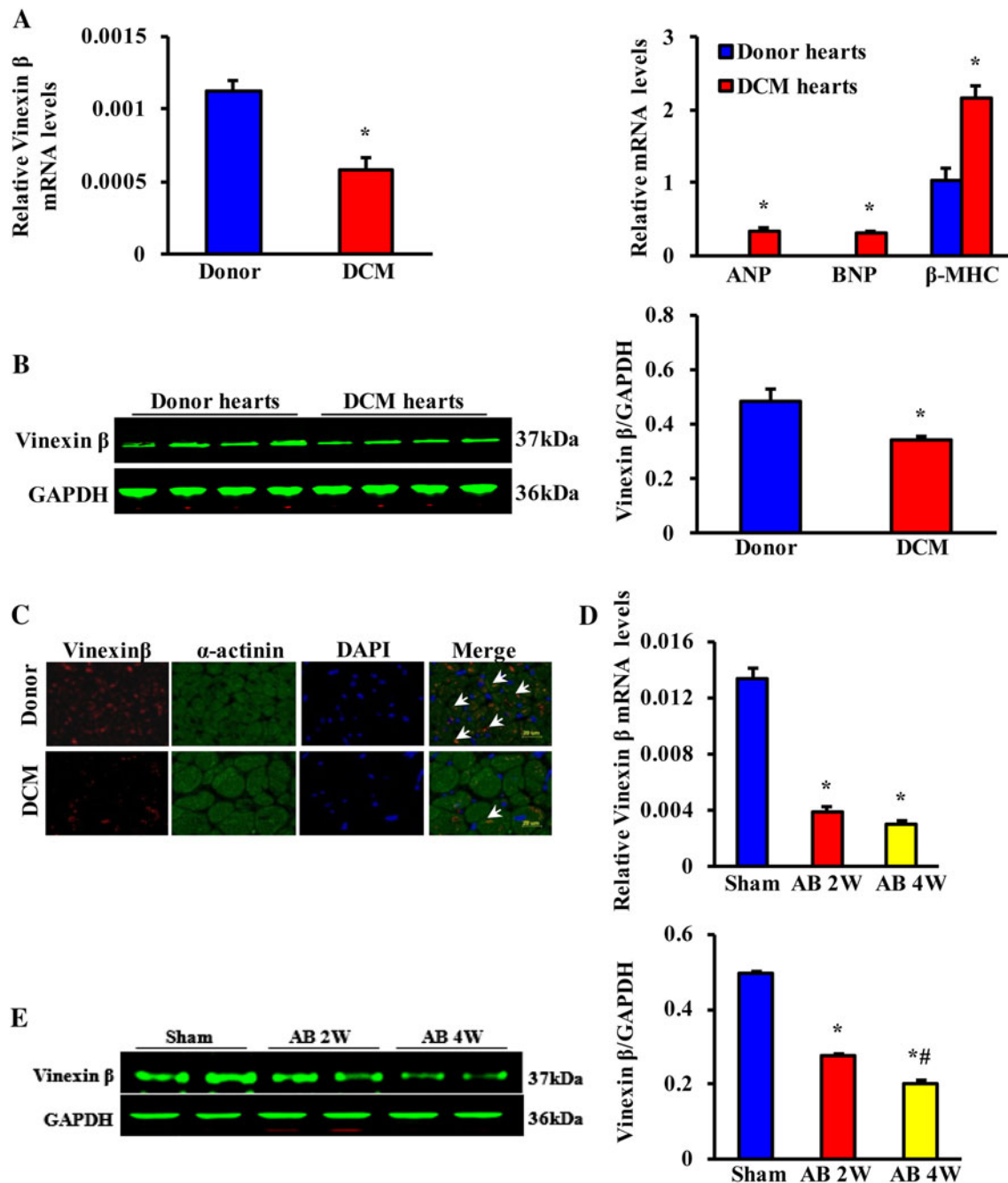
Fig. 1 Vinexin-β expression in failing human hearts and experimental hypertrophic models. **a** Real-time PCR analysis of Vinexin-β, ANP, BNP, and β-MHC in human failing ($n = 4$) and donor hearts ($n = 4$). **b** Representative Western blots of Vinexin-β in the hearts of normal donors ($n = 5$) and patients with heart failure ($n = 5$). **c** Immunofluorescence of the cardiac Vinexin-β protein in human failing ($n = 4$) and donor hearts ($n = 4$). **d** Real-time PCR analysis of Vinexin-β in WT hearts after AB at the indicated time points ($n = 4$). **e** Representative Western blots of Vinexin-β in WT hearts after AB at the indicated time points ($n = 4$). *$P < 0.05$ vs. normal donors or sham. n indicates number of human hearts or mice hearts per experimental group

and penicillin/streptomycin, in 6-well culture plates coated with fibronectin. After 48 h, the culture medium was replaced with F10 medium containing 0.1 % FCS and 0.1 mM BrdU. Cell viability was determined by measuring the cell number, frequency of contractions, cellular morphology, and trypan blue exclusion. For cell infection, cardiomyocytes were cultured at a density of 1×10^6 cells/well in 6-well plates and exposed to 2×10^8 pfu each of virus in 1 ml of serum-free medium for 24 h. The cells were then washed and incubated in serum-containing medium for 24 h. Subsequently, these myocytes were infected with Ad-Vinexin-β, Ad-shVinexin-β, and/or
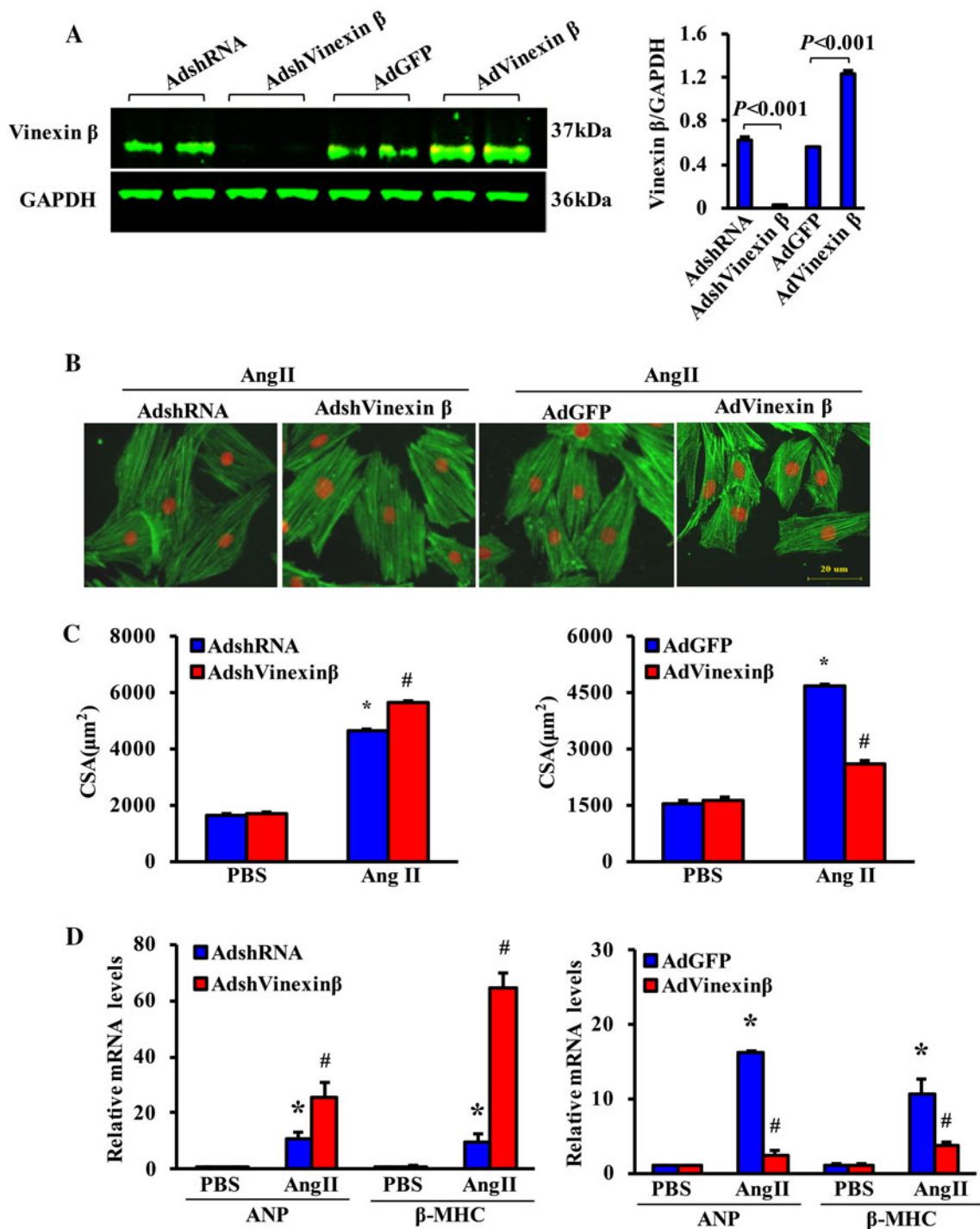
Fig. 2 Effects of Vinexin-β on myocyte hypertrophy in vitro.
a Protein expression levels of Vinexin-β after infection with
Ad-Vinexin-β or Ad-shVinexin-β. *Left panel* representative blots,
right panel quantitative results ($n = 4$, n indicates repeated experi-
ments). **b** Representative images of neonatal rat cardiomyocytes
infected with Ad-shVinexin-β or Ad-Vinexin-β and treated with Ang
II. **c** Analysis of CSA in the indicated groups ($n = 100 \pm$ cells,
n indicates number of cells outlined per experimental group). **d** Real-
time PCR analysis of ANP and β-MHC in neonatal rat cardiomyo-
cytes infected with Ad-shVinexin-β or Ad-Vinexin-β and treated with
PBS or Ang II ($n = 4$, n indicates repeated experiments). *$P < 0.05$
vs. Ad-shRNA or Ad-GFP/PBS. #$P < 0.05$ vs. Ad-shRNA or
Ad-GFP/Ang II

Adca-AKT, Addn-AKT at a MOI of 10 for 12 h. The
culture medium was then replaced with serum-free medium
for 12 h, followed by stimulation with 1 μM Ang II for

48 h. Adca-AKT was purchased from Applied Biological
Materials Inc. (Cat. #000551A), and Addn-AKT was con-
structed in our lab using the AKT dominant-negative

vector (Addgene, Cat. #16243). Additional treatments are described in the figure legends.

Immunofluorescent staining

Immunofluorescent staining was performed in tissue sections or NRCMs with a Vinexin-β antibody to determine the expression levels of Vinexin-β, or with α-actinin antibody to access the CSA. Briefly, cardiac myocytes were infected with different adenoviruses for 24 h and subsequently stimulated with 1 μM Ang II for 48 h. The cells were then fixed with 3.7 % formaldehyde in PBS, permeabilised with 0.1 % Triton X-100 in PBS, and stained with α-actinin at a dilution of 1:100 using standard immunofluorescence staining techniques. For the tissue section staining, the procedure was the same as that used for the NRCM staining after de-parafinisation step (as described above).

Human heart samples

Samples of human failing hearts were collected from the left ventricles of dilated cardiomyopathy (DCM) patients undergoing heart transplants. Control samples were obtained from the left ventricles of normal heart donors who died in accidents but whose hearts were not suitable for transplantation for non-cardiac reasons. Written informed consent was obtained from each DCM patient undergoing transplant and the families of the prospective heart donors. The samples were obtained according to the regulations of the Ethical Committee at the Renmin Hospital of Wuhan University.

Statistical analysis

The data are presented as the mean ± SEM. Differences among groups were determined by a two-way ANOVA followed by a post hoc Tukey test. Comparisons between two groups were performed using an unpaired Student's t test. A value of $P < 0.05$ was considered significant.

Results

Vinexin-β expression in human failing hearts and hypertrophic mouse hearts

To investigate whether Vinexin-β is involved in cardiac hypertrophy, we first examined Vinexin-β expression in the left ventricles of seven DCM patients and six normal donor hearts (Supplementary Table 1). A real-time PCR analysis showed that the levels of Vinexin-β mRNA were decreased

by 48 ± 2 % in the failing DCM hearts, accompanied with increased mRNA levels of foetal genes, such as ANP, BNP, and β-MHC, compared with donor hearts (Fig. 1a). Western blotting and immunostaining analyses consistently demonstrated that the protein levels of Vinexin-β were significantly decreased in the failing human hearts (Fig. 1b, c). We then examined cardiac Vinexin-β expression in response to pressure overload in mice. As expected, the levels of both the Vinexin-β mRNA and protein in the murine hearts progressively decreased over 2–4 weeks after AB (Fig. 1d, e). Together, these findings suggest that Vinexin-β is involved in cardiac hypertrophy.

Effect of Vinexin-β on myocyte hypertrophy in vitro

Next, we employed cultured neonatal rat cardiomyocytes (NRCMs) to examine the possible role of Vinexin-β in modulating myocyte hypertrophy. NRCMs were infected with Ad-Vinexin-β to overexpress Vinexin-β or with Ad-shVinexin-β to knock down endogenous Vinexin-β expression (Fig. 2a). Subsequently, these gene-modified NRCMs were exposed to 1 μM Ang II for 48 h. We observed that Ang II-induced hypertrophy was exaggerated in Ad-shVinexin-β-infected cardiomyocytes, whereas it was alleviated by overexpression of Vinexin-β, as measured by CSA and the mRNA levels of the hypertrophy markers ANP and β-MHC (Fig. 2b, c, d). These results indicate that Vinexin-β may be a negative regulator in Ang II-induced cell hypertrophy.

Characterisation of Vinexin-β knockout mice and cardio-specific transgenic mice

To define the role of Vinexin-β in cardiac hypertrophy in vivo, we generated a transgenic (TG) mouse model with cardiac-specific overexpression of Vinexin-β using the α-myosin heavy chain promoter (Fig. 3a). Western blot analysis demonstrated that Vinexin-β was successfully overexpressed in hearts from four TG mouse lines (Fig. 3b). We then selected the mouse line that expressed the highest levels of Vinexin-β in the heart (Tg.8) for the following studies. Western blotting further confirmed that Vinexin-β was specifically overexpressed in the heart but not in any other tissues/organs (Fig. 3c). In addition, Vinexin-β knockout (KO) mice (provided by the RIKEN BRC, Japan) were utilised in this study (Fig. 3d). The KO and TG mice exhibited normal HW/BW and LW/BW ratios compared with WT mice (Table 1). The degree of fibrosis and the parameters of cardiac contractile function were also similar among the KO, TG, and WT mice (Table 1). Thus, these results indicate that Vinexin-β disruption or overexpression in the heart has no significant impact on normal cardiac growth and function under basal conditions.

Fig. 3 Characterisation of transgenic mice with cardiac-specific Vinexin-β expression and global knockout mice. **a** Schematic diagram of the α-MHC-Vinexin-β transgene construct. **b** Representative Western blots of human Vinexin-β expression in the heart tissue from four TG *lines* and WT mice (*n* = 4). **c** Representative Western blots of transgene Vinexin-β expression in various tissues from TG mice as indicated (*n* = 3). **d** Representative Western blots showing that Vinexin-β is absent in the heart tissue of Vinexin-β knockout mice (*n* = 4). *n* indicates number of mice per experimental group
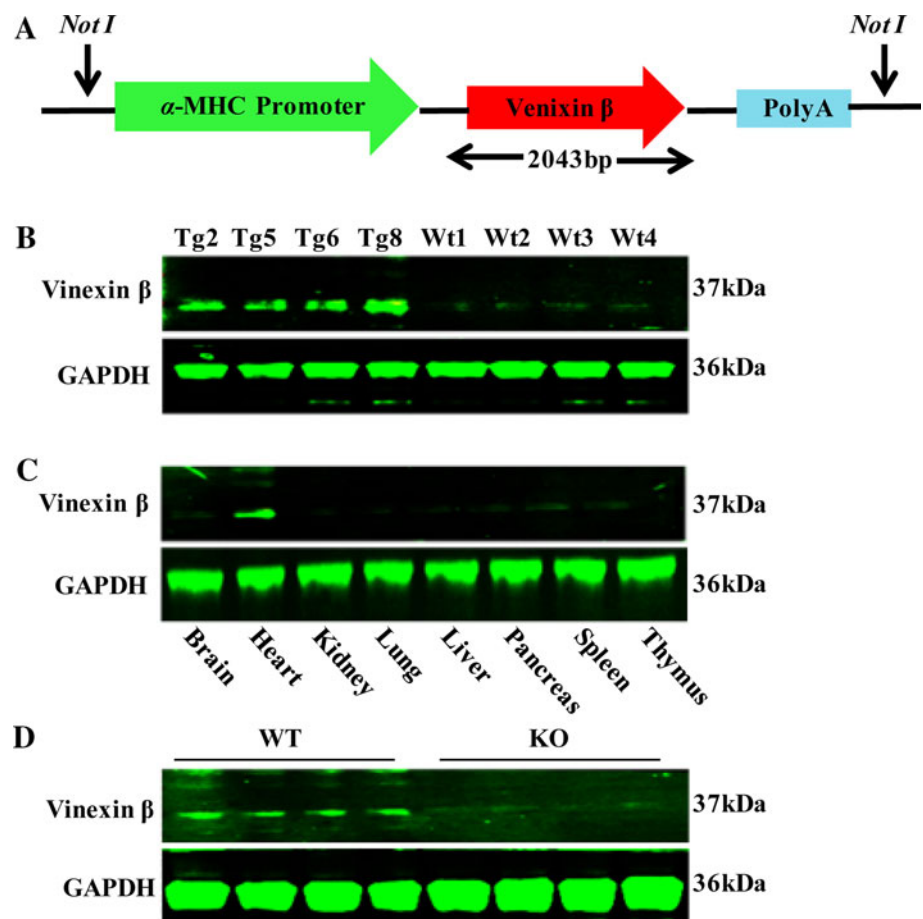
Table 1 Characterisation of Vinexin-β knockout mice and cardiac-specific transgenic mice

Parameter	Vinexin$^{+/+}$	Vinexin$^{-/-}$	NTG	TG
Mice (*n*)	12	13	10	12
BP (mmHg)	78.9 ± 5.0	81.3 ± 4.0	79.3 ± 2.9	82.5 ± 3.0
HW/BW (mg/g)	4.38 ± 0.10	4.22 ± 0.11	4.28 ± 0.10	4.17 ± 0.09
LW/BW (mg/g)	5.35 ± 0.12	5.17 ± 0.10	5.24 ± 0.13	5.15 ± 0.14
HW/TL (mg/mm)	6.49 ± 0.09	6.26 ± 0.12	6.42 ± 0.12	6.22 ± 0.12
HR (bpm)	557.00 ± 23.70	565.40 ± 17.86	522.40 ± 26.24	535.20 ± 21
IVSd (mm)	0.64 ± 0.02	0.67 ± 0.01	0.62 ± 0.02	0.68 ± 0.02
LVEDd (mm)	3.60 ± 0.05	3.68 ± 0.06	3.70 ± 0.07	3.70 ± 0.04
LVPWd (mm)	0.65 ± 0.01	0.70 ± 0.01	0.63 ± 0.01	0.66 ± 0.02
IVSs (mm)	1.02 ± 0.01	1.01 ± 0.02	1.00 ± 0.00	1.06 ± 0.03
LVESd (mm)	2.05 ± 0.04	2.10 ± 0.07	2.07 ± 0.03	2.12 ± 0.09
LVPWs (mm)	1.03 ± 0.02	1.10 ± 0.00	1.05 ± 0.02	1.04 ± 0.03
EF (%)	80.83 ± 0.98	80.00 ± 1.90	80.40 ± 1.33	80.20 ± 0.66
FS (%)	43.67 ± 0.84	43.00 ± 1.89	43.20 ± 1.20	42.80 ± 0.73

Effect of Vinexin-β deficiency on cardiac hypertrophy in vivo

We first determined the effects of Vinexin-β-null on chronic pressure overload-induced cardiac hypertrophy. To this end, Vinexin-β KO and control WT mice were subjected to AB for 2 weeks (note: longer AB caused most of the instances of KO mouse death; thus, 2-week AB was selected for study). As a control, some mice underwent a sham operation. The results of the gross heart, HE and
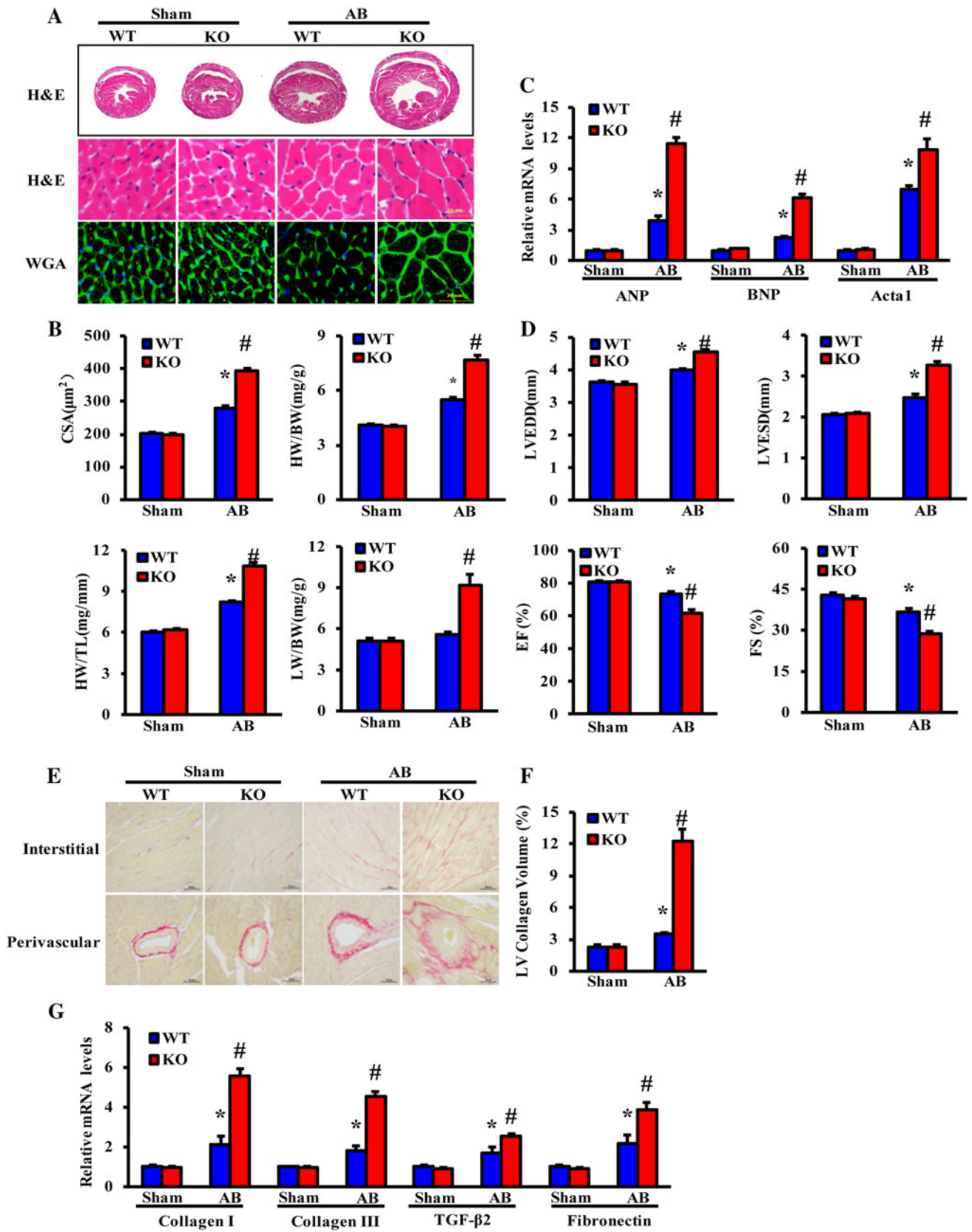
◀ **Fig. 4** Effects of Vinexin-β deficiency on cardiac hypertrophy. **a** Gross hearts, HE and WGA–FITC staining 2 weeks after sham or AB surgery. **b** Statistical results of the myocyte CSA ($n = 100 \pm$ cells, n indicates number of cells outlined per experimental group) and HW/BW, LW/BW and HW/TL ratios ($n = 12$–14, n indicates number of mice per experimental group) of the indicated groups. **c** The AB-induced expression of hypertrophic markers (ANP, BNP, and Acta1) was determined by real-time PCR analysis in WT and KO mice ($n = 4$, n indicates number of mice per experimental group). **d** Echocardiography results for the measurement of myocardial function in WT and KO mice ($n = 8$–9, n indicates number of mice per experimental group). **e** PSR staining of histological LV sections was performed on the indicated groups 2 weeks after AB. **f** Fibrotic areas in the histological sections were quantified using an image analysis system ($n = 5$, n indicates number of mice per experimental group). **g** A real-time PCR analysis was performed to determine mRNA expression levels of collagen I, collagen III, TGF-β2, and fibronectin in the indicated mice ($n = 4$, n indicates number of mice per experimental group). $*P < 0.05$ vs. WT/sham; $^{\#}P < 0.05$ vs. WT/AB

WGA–FITC staining displayed an exaggerated hypertrophic effect of Vinexin-β deficiency on cardiac remodelling after AB (Fig. 4a). Furthermore, the cell CSA and the ratios of HW/BW, HW/TL, and LW/BW were significantly increased in the KO mice compared with the WT mice upon 2-week AB (Fig. 4b). Consistently, the induction of hypertrophic marker expression, e.g., ANP, BNP and Acta1, was significantly enhanced in the KO mice compared with the WT mice after AB (Fig. 4c). As a result, the KO mice exhibited aggravated cardiac dilation and dysfunction compared with the WT mice, as evidenced by echocardiograph parameters, e.g., LVEDD, LVESD, LVEF, and LVFS (Fig. 4d).

Fibrosis is a classic feature of pathological cardiac hypertrophy, which is characterised by the accumulation of collagen in the heart. We therefore examined the effect of Vinexin-β-null on cardiac fibrosis following 2-week aortic banding. As shown in Fig. 4e, marked perivascular and interstitial fibrosis were observed in the WT mice after AB, but these features were remarkably aggravated in KO hearts. The quantitative results showed an increased collagen volume in KO hearts compared with WT hearts (Fig. 4f). Accordingly, the mRNA levels of known fibrosis mediators, including collagen I, collagen III, transforming growth factor (TGF)-β2, and fibronectin, were remarkably elevated in KO hearts compared with WT hearts, indicating a pronounced fibrotic response in the KO mice (Fig. 4g). Taken together, these data suggest that Vinexin-β deficiency promotes cardiac hypertrophy and dysfunction in response to pressure overload.

Effect of Vinexin-β overexpression on cardiac hypertrophy in vivo

To further determine the effect of Vinexin-β overexpression on cardiac hypertrophy, we applied 8-week AB to Vinexin-β TG mice. Histological analysis from gross heart examinations and HE and WGA–FITC staining demonstrated an inhibitory effect of Vinexin-β on cardiac hypertrophy after AB (Fig. 5a). Moreover, Vinexin-β-mediated anti-hypertrophic effects were also evidenced by a reduced CSA and HW/BW, HW/TL, and LW/BW ratios (Fig. 5b). In addition, the mRNA levels of hypertrophic markers (i.e., ANP, BNP and Acta1) in the TG mice were significantly decreased compared with the NTG mice after AB (Fig. 5c). The increase in the LV chamber dimension and the decrease in the LVEF and LVFS induced by pressure overload were also markedly attenuated in the TG mice compared with the NTG mice (Fig. 5d). Next, we examined the effects of Vinexin-β overexpression on cardiac fibrosis and observed that AB-induced perivascular and interstitial fibrosis were attenuated in the TG mice compared with their NTG littermates (data not shown). Such an anti-fibrotic effect of Vinexin-β was supported by subsequent analysis of collagen volume and fibrosis marker expression (collagen I and III, TGF-β and fibronectin) (data not shown). Together, these data clearly suggest that overexpression of Vinexin-β protects against pressure overload-induced cardiac hypertrophy and failure.

Effect of Vinexin-β overexpression on the AKT signalling pathway

To explore the molecular mechanisms underlying Vinexin-β-mediated anti-hypertrophy, we first examined the effect of Vinexin-β overexpression on the MAPK signalling cascade. We found that the degree of AB-induced activation of MEK1/2, ERK1/2, and p38 was similar between groups (KO vs. WT, and TG vs. NTG; data not shown). Given that the AKT cascade is another important signalling pathway involved in cardiac hypertrophy, we then determined whether Vinexin-β affects the AB-induced AKT signalling response. Activation of AKT and its downstream targets, including GSK3β and forkhead box O3A (FOXO3A), were examined in KO and WT hearts. Western blot analysis revealed that Vinexin-β deficiency significantly enhanced the AB-induced phosphorylation of AKT, GSK3β, and FOXO3A (Fig. 6a, b). Conversely, the AB-induced elevation of phosphorylated AKT and its downstream targets were markedly abrogated in the TG hearts compared with the non-TG hearts (Fig. 6c, d). These data suggest that the anti-hypertrophic effect of Vinexin-β may be mediated by the inhibition of the AKT signalling pathway rather than the MAPK pathway. To further confirm the inhibitory effect of Vinexin-β on AKT signalling, we infected neonatal rat cardiomyocytes with
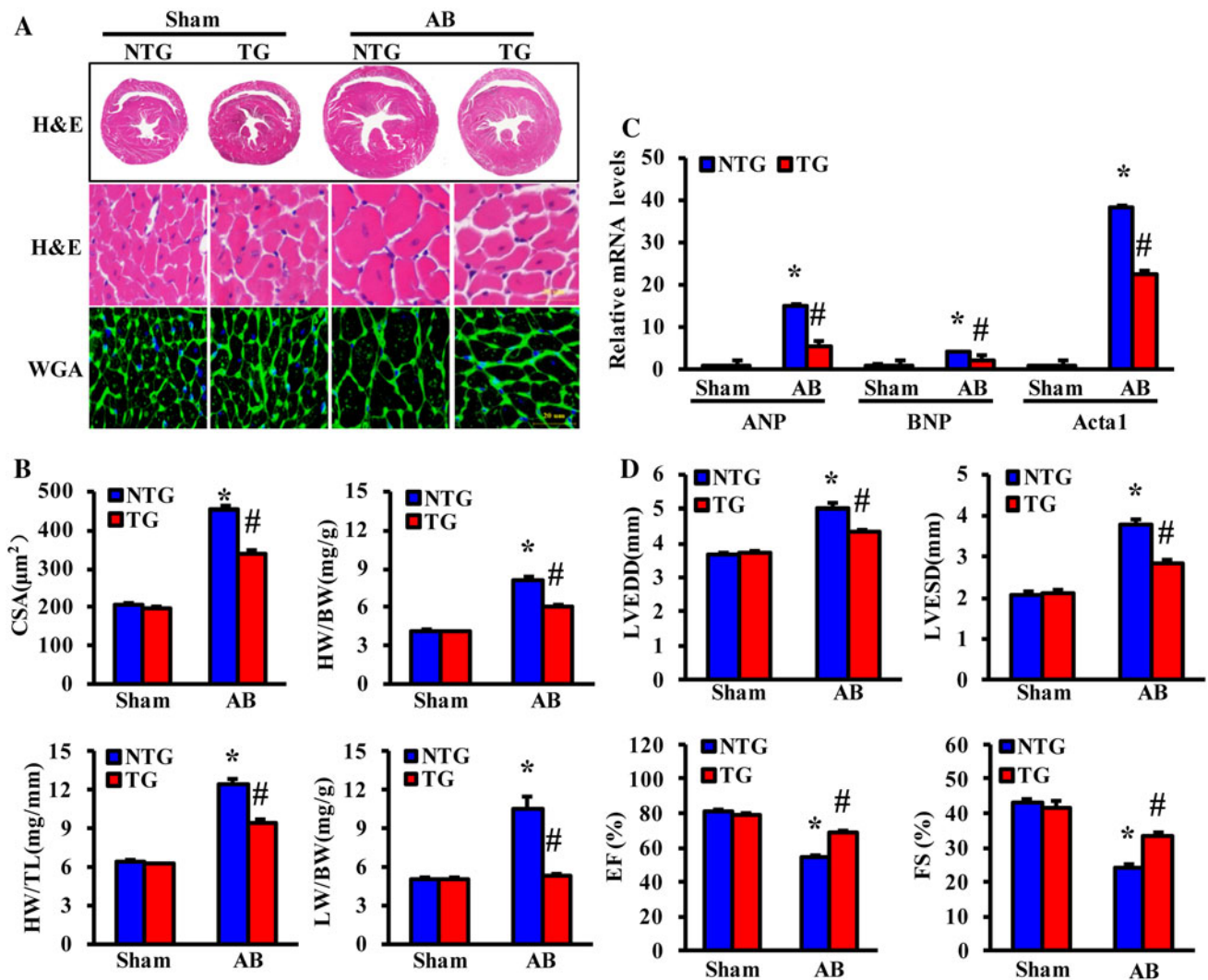
Fig. 5 Effects of Vinexin-β overexpression on cardiac hypertrophy. **a** Gross hearts, HE and WGA–FITC staining in the indicated mice 8 weeks after sham or AB surgery. **b** Statistical results for the myocyte CSA ($n = 100 \pm$ cells, n indicates number of cells outlined per experimental group) and HW/BW, LW/BW and HW/TL ratios ($n = 11–15$, n indicates number of mice per experimental group) of the indicated groups. **c** The AB-induced expression of hypertrophic markers was determined by real-time PCR in NTG and TG mice ($n = 4$, n indicates number of mice per experimental group). **d** Echocardiography results for myocardial function measurements in NTG and TG mice ($n = 11–15$, n indicates number of mice per experimental group). $*P < 0.05$ vs. NTG/sham; $^{\#}P < 0.05$ vs. NTG/AB

Ad-Vinexin-β, Ad-GFP, Ad-shVinexin-β, or Ad-shRNA and then exposed the cells to 1-μM Ang II for 48 h. The Western blotting results showed that the Ang II-triggered activation of AKT/GSK3β/FOXO3A was significantly attenuated by infection with Ad-Vinexin-β (overexpression) but was promoted by infection with Ad-shVinexin-β (knockdown) (Fig. 6e, f, g, h). Taken together, these results indicate that Vinexin-β blocks the AKT signalling activated by Ang II in cardiomyocytes.

To determine whether the anti-hypertrophic effects of Vinexin-β are dependent on the activation of AKT, we co-infected neonatal rat cardiomyocytes with Ad-shVinexin-β plus Addn-AKT (dominant negative mutation of AKT to inhibit AKT activity), or Ad-Vinexin-β plus Adca-AKT (constitutively active AKT), or Ad-shVinexin-β plus Akt inhibitor (10 μM, LY294002) and then exposed the cells to Ang II for 48 h. The results of the CSA analysis showed that among the shRNA-infected groups (Fig. 6i, left and middle panel, blue bars), Ang II-induced myocyte hypertrophy was attenuated in the Addn-AKT-infected or Akt inhibitor-treated cells compared with the control cells. Specifically, the acceleration of Ang II-induced cell hypertrophy caused by Vinexin-β knockdown was dramatically reduced by the overexpression of dominant negative AKT or treating with Akt inhibitor (Fig. 6i, left and middle panel, red bars). In gain-of-function experiments, we observed that Ang
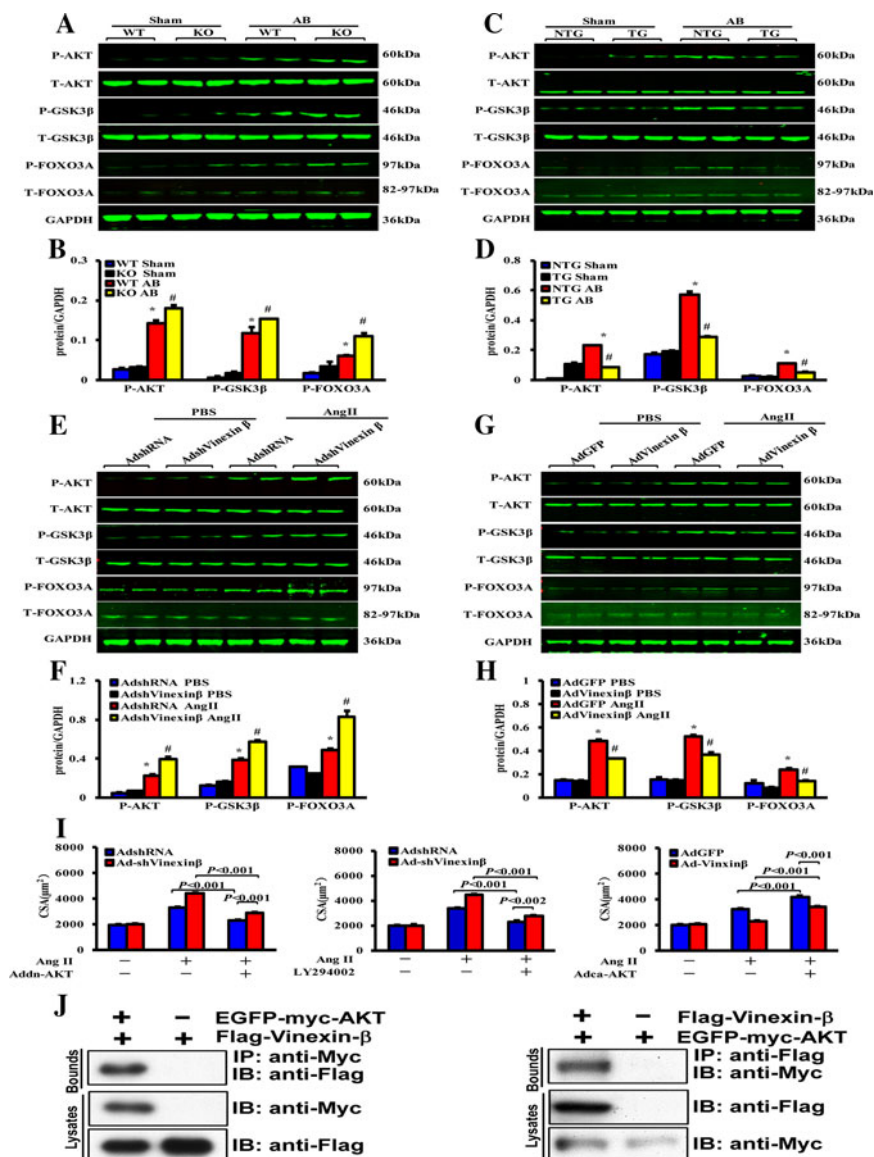
Fig. 6 Effects of Vinexin-β on the AKT signalling pathway. **a** Representative Western blots of total and phosphorylated AKT, GSK3β, and FOXO3A in KO and WT mice 2 weeks after sham or AB surgery. **b** Quantitation of the levels of phosphorylated AKT, GSK3β, and FOXO3A in KO and WT mice ($n = 3$, n indicates number of repeated experiments). *$P < 0.05$ vs. WT/sham; [#]$P < 0.05$ vs. WT/AB. **c** Representative Western blots of total and phosphorylated AKT, GSK3β, and FOXO3A in TG and NTG mice 8 weeks after sham or AB surgery. **d** Quantitation of the levels of phosphorylated AKT, GSK3β, and FOXO3A in TG and NTG mice ($n = 3$, n indicates number of repeated experiments). *$P < 0.05$ vs. NTG/sham; [#]$P < 0.05$ vs. NTG/AB. **e** Representative Western blots of total and phosphorylated AKT, GSK3β, and FOXO3A in neonatal rat cardiomyocytes infected with Ad-shVinexin-β and treated with PBS or Ang II. **f** Quantitation of the levels of phosphorylated AKT, GSK3β, and FOXO3A in the indicated groups after infection with Ad-shVinexin-β and exposure to PBS or Ang II ($n = 3$, n indicates number of repeated experiments). *$P < 0.05$ vs. Ad-shRNA/PBS; [#]$P < 0.05$ vs. Ad-shRNA/Ang II. **g** Representative Western blots of total and phosphorylated AKT, GSK3β, and FOXO3A in neonatal rat cardiomyocytes after infection with Ad-Vinexin-β and exposure to PBS or Ang II. **h** Quantitation of the levels of phosphorylated AKT, GSK3β, and

FOXO3A in the indicated groups after infection with Ad-Vinexin-β and exposure to PBS or Ang II ($n = 3$, n indicates number of repeated experiments). *$P < 0.05$ vs. Ad-GFP/PBS; [#]$P < 0.05$ vs. Ad-GFP/Ang II. **i** *Left panel*: Neonatal rat cardiomyocytes were infected with Ad-shVinexin-β with or without Addn-AKT, followed by treatment with 1 μM Ang II for 48 h. The CSA of the cardiomyocytes was then measured (see "Methods") and revealed that the acceleration of myocyte hypertrophy by Vinexin-β knockdown was attenuated by the overexpression of dominant negative AKT (Addn-AKT). *Middle panel* The Akt inhibitor LY294002 blunted the acceleration of myocyte hypertrophy caused by Vinexin-β knockdown. *Right panel* The Vinexin-β-mediated inhibition of myocyte hypertrophy was promoted by the activation of AKT (Adca-AKT). $n = 100 \pm$ cells, n indicates number of cells outlined per experimental group, *$P < 0.001$ vs. control, respectively. **j** Co-immunoprecipitation experiments showing the physical interaction between Vinexin-β and AKT. HEK293T cells were transiently transfected with the mammalian expression vectors Flag-Vinexin-β and/or EGFP-myc-AKT. The cell lysates were immunoprecipitated with an anti-Myc (*left*) or anti-Flag antibody (*right*) and immunoblotted with an anti-Flag or anti-Myc antibody, respectively

II-induced cell hypertrophy was suppressed by the overexpression of Vinexin-β (Fig. 6i, right panel, red bars). However, the suppression of Ang II-induced cell hypertrophy by the overexpression of Vinexin-β (Fig. 6i, right panel, red bars) was released by the constitutive activation of AKT. Collectively, these data suggest that the regulatory role of Vinexin-β in pathological cardiac hypertrophy is dependent, at least partly, on the activation of AKT. The inhibition of AKT signalling by Vinexin-β prompted us to investigate whether Vinexin-β directly interacts with AKT. Therefore, we constructed plasmids for the expression of Flag-tagged Vinexin-β and EGFP-Myc-labelled AKT. Using co-immunoprecipitation, we observed a direct interaction between Vinexin-β and AKT (Fig. 6j).

Discussion

The major finding of this study is that overexpression of Vinexin-β protects against maladaptive hypertrophy, dilatation, and fibrosis in response to chronic pressure overload, whereas disruption of Vinexin-β expression exaggerates pathological cardiac remodelling and fibrosis. To the best of our knowledge, these findings are the first direct evidence that Vinexin-β plays an important role in modulating maladaptive cardiac remodelling and activating hypertrophic signalling pathways in response to pressure overload.

Vinexin-β expression was significantly downregulated in failing human hearts and hypertrophic mouse hearts. According to our findings that the transgenic overexpression of Vinexin-β in the heart attenuated AB-induced cardiac hypertrophy and fibrosis, whereas loss of Vinexin-β resulted in an exaggerated response of pathological cardiac remodelling, the reduced expression of endogenous Vinexin-β observed in human failing hearts is likely maladaptive. These results strongly suggest that Vinexin-β plays an important role in protecting the heart against maladaptive responses to stress. Nonetheless, how Vinexin-β expression is regulated, especially during the transition from cardiac hypertrophy to failure, is currently unknown. A recent study reported that the mTOR-MEK/ERK pathway is involved in the regulation of Vinexin-β expression in v-Src-transformed cells [38]. Hence, it will be interesting to test whether this pathway affects Vinexin-β expression in the heart.

The anti-hypertrophic effect of Vinexin-β is intriguing. It is generally accepted that a mechanical signal induced by pressure overload will initiate a cascade of biological signalling transduction pathways that increase cardiomyocyte growth and collagen synthesis [9, 10, 12–16, 18, 24, 31, 39, 41, 44]. Previous studies by our group and others have demonstrated that the MAPK pathway is critical in the process of cardiac hypertrophy [2, 3, 28, 33]. The MAPK cascade comprises a sequence of successive kinases,

including p38, JNKs, and ERKs. These kinases directly modify transcription regulatory factors, reprogram cardiac gene expression, and produce cardiac hypertrophy [12]. While previous reports have shown that Vinexin-β modulates the activation of JNK and ERK2 in adherent cells [1, 37]; in the present study, either overexpression or knockdown of Vinexin-β did not alter the levels of phosphorylated ERK1/2 or p38 MAPK in the heart. This result suggests that the regulatory role of Vinexin-β in the MAPK cascade may be tissue/cell dependent. We then examined the AKT signalling pathway (AKT-GSK3β-FOXO), an additional key contributor to the development of cardiac hypertrophy [4, 8, 20, 32]. It has been reported that the activation of AKT and FOXO via phosphorylation produces pro-hypertrophic effects in cardiomyocytes [7, 11]. GSK-3β is a negative regulator of the calcineurin/nuclear factor in activated T cell signalling and cardiac hypertrophy, and it is inactivated by phosphorylation upon hypertrophy stimulation [11]. An important finding from this study is that AKT activation was almost entirely blunted by the cardiac expression of human Vinexin-β, whereas the phosphorylation levels of AKT were further increased by the loss of Vinexin-β expression in response to chronic pressure overload. Consistent with AKT activation, AB induced significant phosphorylation of GSK3β and FOXO, which was attenuated by Vinexin-β overexpression. More importantly, disruption of Vinexin-β expression resulted in a pronounced activation of GSK3β and FOXO. Therefore, AKT signalling is a critical pathway through which Vinexin-β mediates its anti-hypertrophic effect. The identification of AKT as a Vinexin-β-interacting protein in our study suggests that the functional role of Vinexin-β in the heart may be dependent on AKT activation. Consistent with this notion, we observed that overexpression of AKT recovered Vinexin-β-depressed cardiomyocyte hypertrophy, whereas inactivation of AKT suppressed Ad-shVinexin-β-induced hypertrophy, indicating that the inhibitory effects of Vinexin-β on cardiac hypertrophy are largely mediated through AKT signalling. Nonetheless, it should be noted that the induction of cardiac hypertrophy is a result of the triggering of several signal transduction pathways, such as the calcineurin/nuclear factor of activated T cells signalling pathway and the nuclear factor-κB signalling pathway. Therefore, we cannot exclude the possible role of the aforementioned pro-hypertrophic signalling pathways in the mechanism of Vinexin-β.

Currently, there is controversy concerning the regulatory role of AKT in cardiac hypertrophy. Certain investigators have reported that the cardiac-specific overexpression of constitutively active AKT activates downstream targets and promotes cardiac hypertrophy, which is associated with impaired contractile function and interstitial fibrosis [19, 29, 35]. However, additional experiments have produced

different results. For example, Condorelli et al. [5] observed that cardio-selective AKT overexpression significantly increased cardiomyocyte cell size and concentric LV hypertrophy, which was associated with increased cardiac contractility. DeBosch et al. [6] reported that AKT-deficient mice have similar heart weights and cardiac function compared with WT mice. Furthermore, AKT-deficient mice were shown to be resistant to exercise-induced cardiac hypertrophy. In contrast, AKT-deficient mice developed an exacerbated form of cardiac hypertrophy in response to transverse aortic constriction. These observations suggest that AKT is a pivotal regulatory switch that promotes physiological cardiac hypertrophy and antagonises pathological hypertrophy. Using TG mice with cardiac-specific inducible AKT expression, Shiojima et al. [36] showed that short-term AKT activation induces physiological hypertrophy and a moderate increase in heart size, whereas prolonged AKT activation produces pathological hypertrophy with a much larger increase in heart size. Therefore, in the heart, short-term AKT activation induces physiological hypertrophy, whereas long-term AKT activation promotes pathological hypertrophy. Herein, transgenic mice that overexpressed Vinexin-β had markedly blunted AKT signalling, whereas Vinexin-β-deficient mice had significantly enhanced AKT signalling that was induced by 2-week AB. These findings suggest that Vinexin-β may be an endogenous AKT signalling inhibitor.

In conclusion, the work herein is the first evidence that Vinexin-β protects against cardiac hypertrophy and fibrosis in response to pressure overload. The underlying mechanism for the protective role of Vinexin-β in the development of cardiac hypertrophy is related to the inhibition of the AKT signalling pathway. Therefore, we propose that targeting Vinexin-β is a promising approach for treating or preventing cardiac hypertrophy.

References

1. Akamatsu M, Aota S, Suwa A, Ueda K, Amachi T, Yamada KM, Akiyama SK, Kioka N (1999) Vinexin forms a signaling complex with Sos and modulates epidermal growth factor-induced c-Jun N-terminal kinase/stress-activated protein kinase activities. J Biol Chem 274:35933–35937. doi:10.1074/jbc.274.50.35933

2. Bian Z, Cai J, Shen DF, Chen L, Yan L, Tang Q, Li H (2009) Cellular repressor of E1A-stimulated genes attenuates cardiac hypertrophy and fibrosis. J Cell Mol Med 13:1302–1313. doi:10.1111/j.1582-4934.2008.00633.x

3. Braz JC, Bueno OF, Liang Q, Wilkins BJ, Dai YS, Parsons S, Braunwart J, Glascock BJ, Klevitsky R, Kimball TF, Hewett TE, Molkentin JD (2003) Targeted inhibition of p38 MAPK promotes hypertrophic cardiomyopathy through upregulation of calcineurin-NFAT signaling. J Clin Invest 111:1475–1486. doi:10.1172/jci200317295

4. Carneiro-Ramos MS, Diniz GP, Nadu AP, Almeida J, Vieira RL, Santos RA, Barreto-Chaves ML (2010) Blockage of angiotensin II type 2 receptor prevents thyroxine-mediated cardiac hypertrophy by blocking Akt activation. Basic Res Cardiol 105:325–335. doi:10.1007/s00395-010-0089-0

5. Condorelli G, Drusco A, Stassi G, Bellacosa A, Roncarati R, Iaccarino G, Russo MA, Gu Y, Dalton N, Chung C, Latronico MV, Napoli C, Sadoshima J, Croce CM, Ross J Jr (2002) Akt induces enhanced myocardial contractility and cell size in vivo in transgenic mice. Proc Natl Acad Sci USA 99:12333–12338. doi:10.1073/pnas.172376399

6. DeBosch B, Treskov I, Lupu TS, Weinheimer C, Kovacs A, Courtois M, Muslin AJ (2006) Akt1 is required for physiological cardiac growth. Circulation 113:2097–2104. doi:10.1161/CIRCULATIONAHA.105.595231

7. Diniz GP, Carneiro-Ramos MS, Barreto-Chaves ML (2009) Angiotensin type 1 receptor mediates thyroid hormone-induced cardiomyocyte hypertrophy through the Akt/GSK-3beta/mTOR signaling pathway. Basic Res Cardiol 104:653–667. doi:10.1007/s00395-009-0043-1

8. Dorn GW 2nd, Force T (2005) Protein kinase cascades in the regulation of cardiac hypertrophy. J Clin Invest 115:527–537. doi:10.1172/JCI24178

9. Esposito G, Perrino C, Cannavo A, Schiattarella GG, Borgia F, Sannino A, Pironti G, Gargiulo G, di Serafino L, Franzone A, Scudiero L, Grieco P, Indolfi C, Chiariello M (2011) EGFR transactivation by urotensin II receptor is mediated by beta-arrestin recruitment and confers cardioprotection in pressure overload-induced cardiac hypertrophy. Basic Res Cardiol 106:577–589. doi:10.1007/s00395-011-0163-2

10. Garlie JB, Hamid T, Gu Y, Ismahil MA, Chandrasekar B, Prabhu SD (2011) Tumor necrosis factor receptor 2 signaling limits beta-adrenergic receptor-mediated cardiac hypertrophy in vivo. Basic Res Cardiol 106:1193–1205. doi:10.1007/s00395-011-0196-6

11. Hardt SE, Sadoshima J (2002) Glycogen synthase kinase-3beta: a novel regulator of cardiac hypertrophy and development. Circ Res 90:1055–1063. doi:10.1161/01.RES.0000018952.70505.F1

12. Heineke J, Molkentin JD (2006) Regulation of cardiac hypertrophy by intracellular signalling pathways. Nat Rev Mol Cell Biol 7:589–600. doi:10.1038/nrm1983

13. Heusch G (2009) Diastolic heart failure: a misNOmer. Basic Res Cardiol 104:465–467. doi:10.1007/s00395-009-0025-3

14. Heusch G (2011) SCIPIO brings new momentum to cardiac cell therapy. Lancet 378:1827–1828. doi:10.1016/S0140-6736(11)61648-6

15. Heusch G, Kleinbongard P, Skyschally A, Levkau B, Schulz R, Erbel R (2012) The coronary circulation in cardioprotection: more than just one confounder. Cardiovasc Res 94:237–245. doi:10.1093/cvr/cvr271

16. Heusch G, Neumann T (1998) Calcium responsiveness in canine pacing-induced heart failure. J Mol Cell Cardiol 30:1605–1613. doi:10.1006/jmcc.1998.0726

17. Heusch G, Schulz R (2011) A radical view on the contractile machinery in human heart failure. J Am Coll Cardiol 57:310–312. doi:10.1016/j.jacc.2010.06.057

18. Heusch P, Canton M, Aker S, van de Sand A, Konietzka I, Rassaf T, Menazza S, Brodde OE, Di Lisa F, Heusch G, Schulz R (2010) The contribution of reactive oxygen species and p38 mitogen-activated protein kinase to myofilament oxidation and progression of heart failure in rabbits. Br J Pharmacol 160:1408–1416. doi:10.1111/j.1476-5381.2010.00793.x

19. Hua Y, Zhang Y, Ceylan-Isik AF, Wold LE, Nunn JM, Ren J (2011) Chronic Akt activation accentuates aging-induced cardiac hypertrophy and myocardial contractile dysfunction: role of autophagy. Basic Res Cardiol 106:1173–1191. doi:10.1007/s00395-011-0222-8

20. Huang H, Tang QZ, Wang AB, Chen M, Yan L, Liu C, Jiang H, Yang Q, Bian ZY, Bai X, Zhu LH, Wang L, Li H (2010) Tumor suppressor A20 protects against cardiac hypertrophy and fibrosis by blocking transforming growth factor-beta-activated kinase 1-dependent signaling. Hypertension 56:232–239. doi:10.1161/HYPERTENSIONAHA.110.149963

21. Kioka N, Sakata S, Kawauchi T, Amachi T, Akiyama SK, Okazaki K, Yaen C, Yamada KM, Aota S (1999) Vinexin: a novel vinculin-binding protein with multiple SH3 domains enhances actin cytoskeletal organization. J Cell Biol 144:59–69. doi:10.1083/jcb.144.1.59

22. Kioka N, Ueda K, Amachi T (2002) Vinexin, CAP/ponsin, ArgBP2: a novel adaptor protein family regulating cytoskeletal organization and signal transduction. Cell Struct Funct 27:1–7

23. Kovacic-Milivojevic B, Roediger F, Almeida EAC, Damsky CH, Gardner DG, Ilic D (2001) Focal adhesion kinase and p130Cas mediate both sarcomeric organization and activation of genes associated with cardiac myocyte hypertrophy. Mol Biol Cell 12:2290–2307

24. Krusche CA, Holthofer B, Hofe V, van de Sandt AM, Eshkind L, Bockamp E, Merx MW, Kant S, Windoffer R, Leube RE (2011) Desmoglein 2 mutant mice develop cardiac fibrosis and dilation. Basic Res Cardiol 106:617–633. doi:10.1007/s00395-011-0175-y

25. Li H, He C, Feng J, Zhang Y, Tang Q, Bian Z, Bai X, Zhou H, Jiang H, Heximer SP, Qin M, Huang H, Liu PP, Huang C (2010) Regulator of G protein signaling 5 protects against cardiac hypertrophy and fibrosis during biomechanical stress of pressure overload. Proc Natl Acad Sci USA 107:13818–13823. doi:10.1073/pnas.1008397107

26. Li HL, Zhuo ML, Wang D, Wang AB, Cai H, Sun LH, Yang Q, Huang Y, Wei YS, Liu PP, Liu DP, Liang CC (2007) Targeted cardiac overexpression of A20 improves left ventricular performance and reduces compensatory hypertrophy after myocardial infarction. Circulation 115:1885–1894. doi:10.1161/CIRCULATIONAHA.106.656835

27. Lorell BH, Carabello BA (2000) Left ventricular hypertrophy: pathogenesis, detection, and prognosis. Circulation 102:470–479. doi:10.1161/01.CIR.102.4.470

28. Lu J, Bian ZY, Zhang R, Zhang Y, Liu C, Yan L, Zhang SM, Jiang DS, Wei X, Zhu XH, Chen M, Wang AB, Chen Y, Yang Q, Liu PP, Li H (2013) Interferon regulatory factor 3 is a negative regulator of pathological cardiac hypertrophy. Basic Res Cardiol 108:326. doi:10.1007/s00395-012-0326-9

29. Matsui T, Li L, Wu JC, Cook SA, Nagoshi T, Picard MH, Liao R, Rosenzweig A (2002) Phenotypic spectrum caused by transgenic overexpression of activated Akt in the heart. J Biol Chem 277:22896–22901. doi:10.1074/jbc.M200347200

30. Matsuyama M, Mizusaki H, Shimono A, Mukai T, Okumura K, Abe K, Shimada K, Morohashi K (2005) A novel isoform of Vinexin, Vinexin gamma, regulates Sox9 gene expression through activation of MAPK cascade in mouse fetal gonad. Genes Cells 10:421–434. doi:10.1111/j.1365-2443.2005.00844.x

31. Miller CL, Cai Y, Oikawa M, Thomas T, Dostmann WR, Zaccolo M, Fujiwara K, Yan C (2011) Cyclic nucleotide phosphodiesterase 1A: a key regulator of cardiac fibroblast activation and extracellular matrix remodeling in the heart. Basic Res Cardiol 106:1023–1039. doi:10.1007/s00395-011-0228-2

32. Miyamoto T, Takeishi Y, Takahashi H, Shishido T, Arimoto T, Tomoike H, Kubota I (2004) Activation of distinct signal transduction pathways in hypertrophied hearts by pressure and volume overload. Basic Res Cardiol 99:328–337. doi:10.1007/s00395-004-0482-7

33. Molkentin JD (2004) Calcineurin-NFAT signaling regulates the cardiac hypertrophic response in coordination with the MAPKs. Cardiovasc Res 63:467–475. doi:10.1016/j.cardiores.2004.01.021

34. Ruilope LM, Schmieder RE (2008) Left ventricular hypertrophy and clinical outcomes in hypertensive patients. Am J Hypertens 21:500–508. doi:10.1038/ajh.2008.16

35. Shioi T, McMullen JR, Kang PM, Douglas PS, Obata T, Franke TF, Cantley LC, Izumo S (2002) Akt/protein kinase B promotes organ growth in transgenic mice. Mol Cell Biol 22:2799–2809. doi:10.1128/MCB.22.8.2799-2809.2002

36. Shiojima I, Sato K, Izumiya Y, Schiekofer S, Ito M, Liao R, Colucci WS, Walsh K (2005) Disruption of coordinated cardiac hypertrophy and angiogenesis contributes to the transition to heart failure. J Clin Invest 115:2108–2118. doi:10.1172/JCI24682

37. Suwa A, Mitsushima M, Ito T, Akamatsu M, Ueda K, Amachi T, Kioka N (2002) Vinexin beta regulates the anchorage dependence of ERK2 activation stimulated by epidermal growth factor. J Biol Chem 277:13053–13058. doi:10.1074/jbc.M108644200

38. Umemoto T, Inomoto T, Ueda K, Hamaguchi M, Kioka N (2009) v-Src-mediated transformation suppresses the expression of focal adhesion protein vinexin. Cancer Lett 279:22–29. doi:10.1016/j.canlet.2009.01.017

39. Wenzel S, Henning K, Habbig A, Forst S, Schreckenberg R, Heger J, Maxeiner H, Schluter KD (2010) TGF-beta1 improves cardiac performance via up-regulation of laminin receptor 37/67 in adult ventricular cardiomyocytes. Basic Res Cardiol 105:621–629. doi:10.1007/s00395-010-0108-1

40. Xiao J, Moon M, Yan L, Nian M, Zhang Y, Liu C, Lu J, Guan H, Chen M, Jiang D, Jiang H, Liu PP, Li H (2012) Cellular FLICE-inhibitory protein protects against cardiac remodelling after myocardial infarction. Basic Res Cardiol 107:239. doi:10.1007/s00395-011-0239-z

41. Xu Z, Desai M, Philip J, Sivsubramanian N, Bowles NE, Vallejo JG (2011) Conditional transgenic expression of TIR-domain-containing adaptor-inducing interferon-beta (TRIF) in the adult mouse heart is protective in acute viral myocarditis. Basic Res Cardiol 106:1159–1171. doi:10.1007/s00395-011-0226-4

42. Yan L, Wei X, Tang QZ, Feng J, Zhang Y, Liu C, Bian ZY, Zhang LF, Chen M, Bai X, Wang AB, Fassett J, Chen Y, He YW, Yang Q, Liu PP, Li H (2011) Cardiac-specific mindin overexpression attenuates cardiac hypertrophy via blocking AKT/GSK3beta and TGF-beta1-Smad signalling. Cardiovasc Res 92:85–94. doi:10.1093/cvr/cvr159

43. Zhang S, Weinheimer C, Courtois M, Kovacs A, Zhang CE, Cheng AM, Wang Y, Muslin AJ (2003) The role of the Grb2-p38 MAPK signaling pathway in cardiac hypertrophy and fibrosis. J Clin Invest 111:833–841. doi:10.1172/JCI16290

44. Zhu Y, Li T, Song J, Liu C, Hu Y, Que L, Ha T, Kelley J, Chen Q, Li C, Li Y (2011) The TIR/BB-loop mimetic AS-1 prevents cardiac hypertrophy by inhibiting IL-1R-mediated MyD88-dependent signaling. Basic Res Cardiol 106:787–799. doi:10.1007/s00395-011-0182-z